Darko Veljić[1], Walid Musrati[2], Bojan Međo[3], Aleksandar Sedmak[4], Nenad Radović[3]*

NUMERICAL SIMULATION OF FRICTION STIR WELDING - THE PLUNGE STAGE IN T-JOINT

NUMERIČKA SIMULACIJA ZAVARIVANJA TRENJEM SA MEŠANJEM - FAZA URANJANJA ALATA U T-SPOJ

Originalni naučni rad / Original scientific paper
UDK /UDC:

Rad primljen / Paper received: 15.03.2024

Adresa autora / Author's address:
[1)] University of Belgrade, Innovation Centre of the Faculty of Technology and Metallurgy, Belgrade, Serbia
[*]email: dveljic@tmf.bg.ac.rs
[2)] University of El Mergib, Faculty of Engineering, Khoms, Libya
[3)] University of Belgrade, Faculty of Technology and Metallurgy, Belgrade, Serbia
[4)] University of Belgrade, Faculty of Mechanical Engineering, Belgrade, Serbia

Keywords
- friction stir welding
- numerical simulation
- temperature field
- tool pin

Ključne reči
- zavarivanje trenjem sa mešanjem
- numerička simulacija
- temperaturno polje
- trn alata

Abstract

This paper deals with the tool plunge stage of friction stir welding which precedes the formation of the T-joint. A three-dimensional numerical model, developed in software package Simulia Abaqus® is applied for numerical analysis. The material of the welding plates is high strength aluminium alloy 2024-T3 of 3 mm thickness. The change of thermomechanical conditions in the welding zones has been analysed, as well as the conditions for eliminating the joining line in the weld root. The tool rotation speed and shoulder plunge depth are varied. Two tools are used for analysis with different tool pin lengths: 2.6 mm and 3 mm. Increase in tool rotation speed raises the temperature in the welding zone and creates conditions for eliminating the joining line in the weld root. In addition, the increased tool pin length is also beneficial. It is obtained that the tool rotation speed exceeding 500 min^{-1} is necessary for this joint and tool geometries.

Izvod

U ovom radu je analizirana faza uranjanja alata pri formiranju T spoja primenom postupka zavarivanja trenjem sa mešanjem. Za termomehaničku analizu je korišćen trodimenzionalni numerički model, razvijen u softverskom paketu Abaqus®. Radne ploče su od legure aluminijuma visoke čvrstoće 2024-T3, debljine 3 mm. Praćena je promena termomehaničkih uslova u zoni zavarivanja tokom uranjanja alata, kao i uslovi potrebni za eliminisanje linije spajanja u korenom delu zavara. Menjana je brzina rotacije alata i dubina uranjanja čela alata. Za analizu su korišćeni alati sa dužinom trna 2.6 mm i 3 mm. Povećanjem brzine rotacije alata, povećava se temperatura u zoni zavarivanja i stvaraju se uslovi za eliminisanje linije spajanja u korenu zavara. Povećanje dužine trna alata utiče na eliminisanje linije spajanja. Prema dobijenim rezultatima, brzina rotacije iznad 500 min^{-1} je potrebna za razmatrane geometrije spoja i alata.

INTRODUCTION

Friction stir welding (FSW) is one of the most efficient procedures for solid state joining. The heat is generated due to the direct transformation of mechanical energy onto the contact surface tool-sample. Therefore, FSW is a solid state joining process where combination of heat and mechanical work leads to high-quality joints without defects. This method is mostly applied for welding of high strength aluminium alloys for industrial production of airplanes, cars, trains, and ships. From the very beginning, the experimental development of friction stir welding has been accompanied by numerical modelling; some examples are studies /1-4/.

In addition to classical butt welding, a need for different other geometries for manufacturing complex-shaped structural elements often emerges; one of the most frequently applied geometries is the T-joint. Figure 1 contains several design solutions for the formation of T-joints by friction stir welding, /5/.

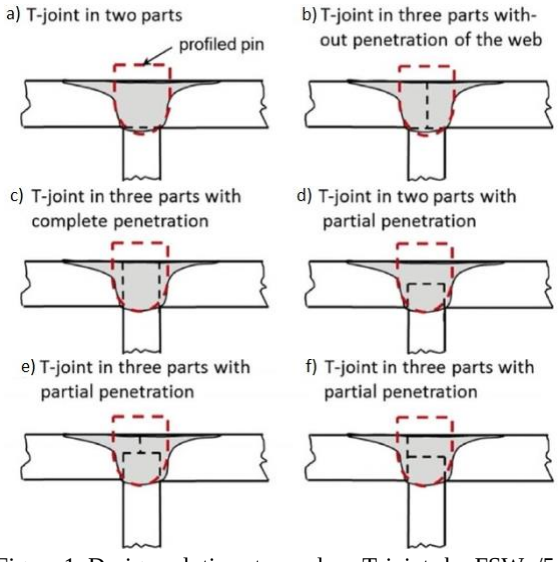

Figure 1. Design solutions to produce T-joints by FSW, /5/.

Many studies have dealt with different aspects of T-joints fabricated by FSW from different materials; a brief overview of a selection of recent works is given here. In a recent work, a detailed examination of friction stir welding of T-joints from Al alloy AA6063-T6 is shown, /6/. Experimental and statistical analysis is performed, and it is shown that the tool rotation speed, tool translation speed, and axial force are significant to the mechanical properties in all joint zones.

The microstructure and hardness profiles in the friction stir welded T-joints of AA6061-T4 sheets are analysed in /7/, in two configurations: T-butt and T-lap joint. Distribution and size of original joint line with severe deformation (OJL wSD) defect was examined. Joint efficiency was determined for both geometries, and the lowest values are obtained for the stringer of the T-lap joint.

In the study /8/, the influence of a second welding pass on the properties of AA5083 FSW T-joints was evaluated. In the second pass, the tool rotation direction remains unchanged, while the translation is in the opposite direction with respect to the first pass. The authors concluded that the second pass has a significant influence on thermo-mechanical conditions, and subsequently on mechanical properties of the FSW joint. Fabrication and examination of FSW T-joints are shown in /9, 10/, including an analysis of mechanical properties of the joints and defects occurring in them.

An important feature, the angle of the tool with respect to the welded piece (tilt angle) is varied in /11/. Numerical modelling is applied through the CFD approach, where the welded plates are considered as non-Newtonian fluid with visco-plastic behaviour. A range of the tilt angle values is obtained in which incomplete joints, as well as the tunnelling effect, are avoided.

The influence of tool geometry, welding parameters, and joint configuration on the quality of dissimilar T-joints made by FSW on AA5083-H111 and 6082-T6 is analysed in /12/. Joint configuration (T-butt and T-lap) does not affect the microstructure and hardness significantly, but T-butt is obtained to be less prone to weld defects. The authors also compared the fatigue behaviour of the FSW joints and those produced by MIG welding, concluding that the FSW joints are superior. Dissimilar Al-alloy joints are also analysed in another recent paper, /13/, where corner stationary-shoulder friction stir welding is applied. This technique is particularly well-suited for T-joints, having in mind that the tool enables joining of two plates perpendicular to each other.

Another group of materials which can be welded by friction stir welding are titanium and its alloys. Microstructure, texture, and mechanical properties in Ti-4Al-0.005B (TA5, Chinese grade) T-joint are examined in /14/. A comparison of fatigue performance of joints produced from the same alloy, but using different friction stir welding sequences, including the application of double weld, is shown in /15/. Fatigue of T-joints is also analysed in /16/, on the example of the AA2024 T351 alloy FSW joint.

Friction stir weldability of Ti6Al4V T-joints with complete penetration is presented in /17/. The authors obtained very good properties of the welds, with some minor flaws present in all joints. Also, wearing of the welding tool is reported in this work as a serious problem for the analysed alloy, although it did not cause a significant decrease of the joint properties.

Just like in most conventional welding procedures, post-weld treatments can be applied to improve the properties of FSW joints; an example is presented in /18/ for AA6063 joints. The authors mention a significant decrease of the grain size during welding, from 47.3 μm to 2.6 μm. Subsequent PWHT increased the mechanical properties of the joints.

As for the numerical analysis, simulation of the friction stir welding of aluminium 6061-T6 alloy T-joint is presented in /19/. Johnson-Cook material model is applied, and the temperature, energy, and reaction force were tracked during the plunge and linear welding stage. Simulation of a different technique, stationary shoulder friction stir welding (CSS FSW), on similar geometries is considered in /20/. This technique was also used in a previously mentioned paper, /13/.

Residual stresses obtained from numerical simulation were the main topic in another work, /21/, on the example of Ti grade 2 joints. The influence of the joint geometry on residual stress distribution is discussed in comparison with the butt joint; T-joint has a unique maximum value, while M-shaped distribution is obtained for butt joint. Also, the authors state that the application of double shoulder tool for the analysed material and geometry results in excessive heat generation and a narrow range of appropriate welding parameters.

Friction stir welding is not used exclusively for metallic materials; e.g., joining of HDPE (high density polyethylene) plates is considered in /22/. Some more recent works deal with hybrid joints, fabricated from a combination of metallic and polymer materials. One such example is /23/, where T-joints are produced from AA5754 aluminium alloy and poly (methyl methacrylate) PMMA. Of course, one of the main issues is the fact that temperatures in the welding zone are likely to exceed the melting temperature of PMMA.

A more common combination of joined materials is steel - aluminium alloy welded joint; such joints are fabricated and examined in numerous works, /24/. The joints were formed in two passes, with steel as the stringer. The authors highlight the importance of the flow lines of the two joining materials, and state that good quality joints are formed if they are in the same direction.

In the study /25/, the main focus is on examination of defect formation in dissimilar Al-alloy T-joints; the main plate was AA8011 aluminium alloy, while the stringer was fabricated from AA5754 alloy. The authors examine the conditions for occurrence of tunnelling and kissing bond defects.

In this work, the tool plunge stage for aluminium alloy 2024-T3 T-joint is analysed. Temperature and von Mises stress fields are used to assess the conditions for elimination of the joining line.

MATERIAL

The material of the welding plates is AA2024-T3. The material of the tool is steel 155CrVMo121 and the material of the backing plate is steel 42CrMo4. The thermal and mechanical properties used in this model are given in Table 1.

Table 1: Material properties of AA2024-T3, /26, 27/.

Material properties	Value
Young's modulus of elasticity (GPa)	73.1
Poisson´s ratio	0.33
Thermal conductivity (W/mK)	121
Coefficient of thermal expansion ($°C^{-1}$)	24.7×10^{-6}
Density (kg/m^3)	2770
Specific heat capacity (J/kg °C)	875
Solidus (°C)	502
Liquidus (°C)	638

NUMERICAL MODEL

The numerical model of the T-joint consists of three working plates with dimensions 25×50 mm and thickness 3 mm, positioned as shown in Fig. 2. The tools, Fig. 3, and two backing plates, Fig. 2, are modelled as rigid surfaces having no thermal degrees of freedom. Figure 4 contains the complete numerical model, assembled from the previously mentioned elements.

For the three-dimensional numerical model, a C3D8RT element type is used which is a thermo-mechanically coupled hexahedral element with 8-nodes, each having trilinear displacement and temperature degrees of freedom. This element produces uniform strain (first-order reduced integration) and contains hourglass control.

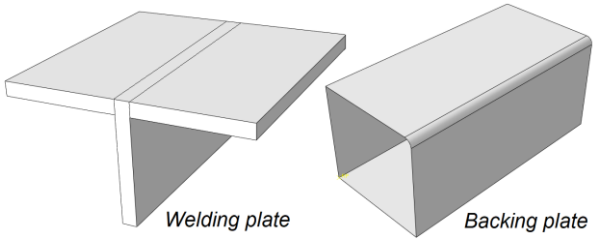

Figure 2. Welding plates and a backing plate.

Only the geometry of the model is described and shown here, since the material model (Johnson-Cook, /28/) and its parameters for the examined alloy are given in the previous works which deal with the plunge stage, but on butt joints /29-33/. The authors have also previously dealt with the linear welding stage in butt joints of the same alloy; some of the works about this topic are /34-36/, where different aspects are covered through experimental and numerical analysis, e.g., welding parameters, material properties, and microstructure of joint zones.

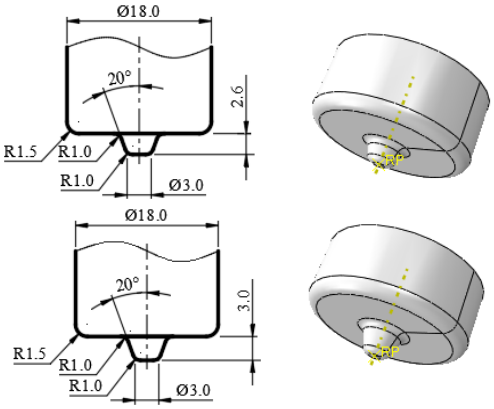

Figure 3. Welding tools - dimensions.

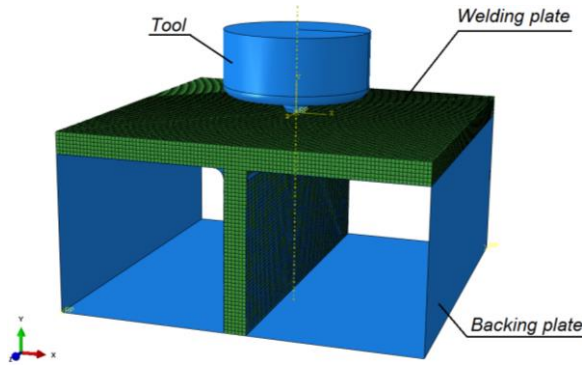

Figure 4. Numerical model of welding plate, tool, and backing plates.

The critical position, having significant influence on the welded joint quality, is shown by the arrow in Fig. 5. It is crucial to set the conditions for eliminating the joining line in the weld root. Two conditions have to be satisfied: material has to reach the temperature of hot plastic processing (about 80 % of melting temperature /37, 38/, around 401 °C for Al alloy 2024 T3), and the distance of the tool tip from the joining line must be within the range 0.1-0.2 mm, /39/.

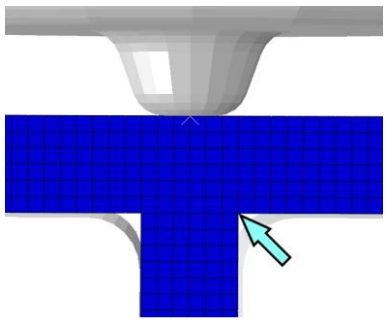

Figure 5. Point where the critical temperature value is tracked.

The cross-section of the working plates is shown in Fig. 6; two tools, with tool pin lengths 2.6 and 3 mm, are considered. Penetration depth of the tool shoulder is 0.2 mm. Tool pin of length 3 mm results in better conditions for eliminating the joining line, because the distance of the tip of the pin from the joining line is 0.1 mm. For pin length 2.6 mm this distance is 0.4 mm, Fig. 6.

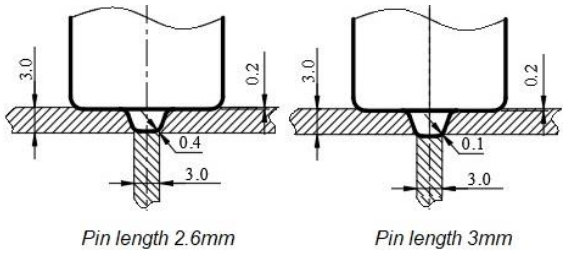

Figure 6. Two tool pin geometries, including the distance from the tip of the pin to the joining line.

By increasing the tool rotation speed, it is possible to enlarge the hot plastic processing zone in the critical area and create conditions for eliminating the joining line in case when the distance between the tip of the pin and joining line is larger than typical.

Plunge stage simulations are performed on T joint for various welding parameters (tool rotation speed 300, 500, 750, and 1000 min^{-1} and tool plunge velocity 0.1 mm/s).

Temperature fields are analysed in the cross-section of the welded joint.

RESULTS AND DISCUSSION

Figures 7-9 show the temperature fields at the surface of the working plates for one selected set of welding parameters. Tool rotation speed is 500 min^{-1}, while tool plunge velocity is 0.1 mm/s. Tool pin length is 3 mm. Penetration depth of the tool shoulder into the material is 0.2 mm, and the process lasted 32 s. Temperature scale is limited up to solidus temperature (T = 502 °C). It can be seen that the temperature fields are symmetrical with respect to the tool axis, which is vertical. At the end of the tool plunge, the material under the tool shoulder is sufficiently heated (401-502 °C).

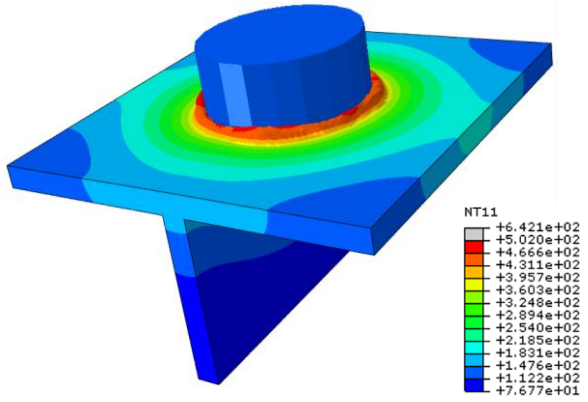

Figure 7. Temperature field after 32 s, pin 3 mm (500 min^{-1}, 0.1 m/s).

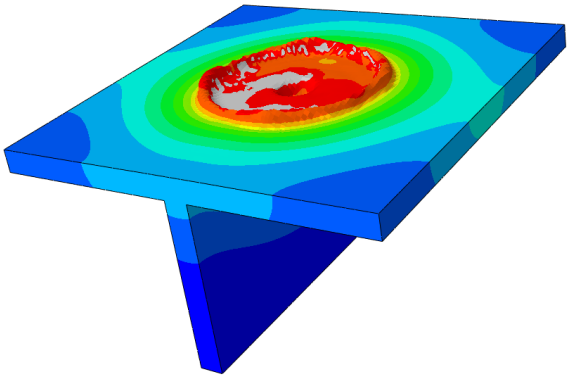

Figure 8. Temperature field after 32 s, pin 3 mm (500 min^{-1}, 0.1 m/s); the same legend as in Fig. 7.

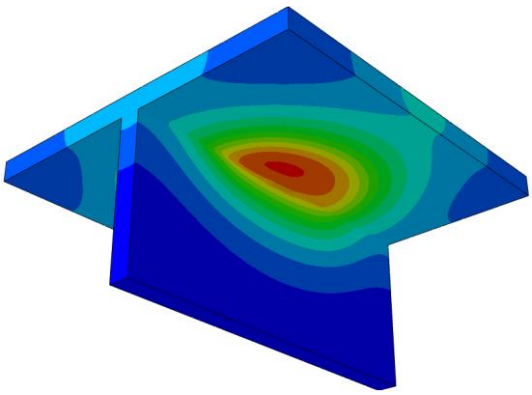

Figure 9. Temperature field after 32 s, pin 3 mm, lower side of the joint (500 min^{-1}, 0.1 m/s); the same legend as in Fig. 7.

Figure 10 shows the temperature field in the cross-section of the welded joint at the end of the plunge stage, after 32 s. The tool rotation speed is 750 min^{-1}, tool plunge velocity is 0.1 mm/s, and tool pin length is 3 mm. Temperature scale maximum is set to 401 °C, the minimal temperature needed for performing friction stir welding on alloy 2024 T3, (as mentioned previously, about 80 % of the material melting temperature, /35, 36/). In the critical part, the necessary material temperature is reached and the tool pin has adequate length. Therefore, it can be said that the conditions for successful friction stir welding, without the occurrence of defects, are satisfied.

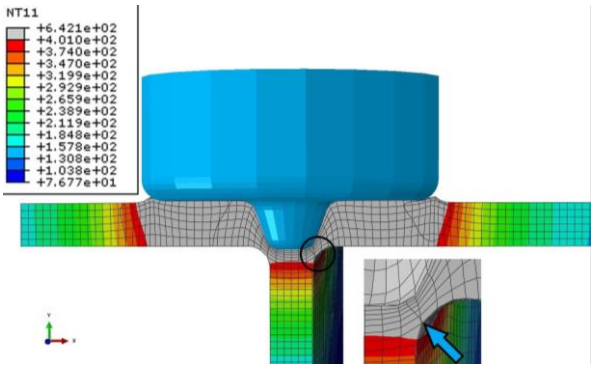

Figure 10. Temperature field after 32 s, pin 3 mm (750 min^{-1}, 0.1 m/s).

Figure 11 shows temperature fields in the critical zone at the end of the tool plunge process, after 32 s. Tool rotation speed is 300, 500, 750 and 1000 min^{-1}, tool plunge velocity is 0.1 mm/s and tool pin length 3 mm. For tool rotation speed of 300 min^{-1}, the temperature condition (401 °C) is not satisfied in the critical position. For 500 min^{-1}, the condition is barely met, while it is satisfied for 750 and 1000 min^{-1}.

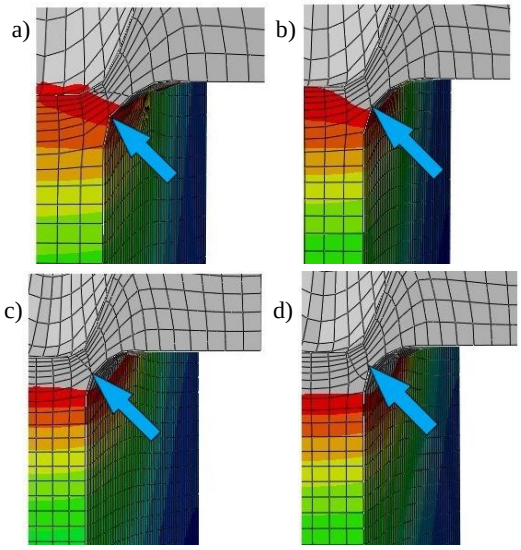

Figure 11. Temperature field after 32 s, pin length 3 mm (300, 500, 750 and 1000 min^{-1}, 0.1 m/s); same legend as in Fig. 10.

Temperature fields in the critical zone for the model with pin length 2.6 mm are shown in Fig. 12. As in the previous figure, these fields are obtained at the end of the tool plunge, which is 28 s for this tool geometry; the rest of the parameters are the same. It can be seen that the temperature condition (reaching 401 °C) is not fulfilled for tool rotation speeds

300 and 500 min^{-1}. As mentioned previously, in this case the distance from pin tip to the critical point is larger than usual; however, the possibility for eliminating the joining line exists for tool rotation speeds 750 and 1000 min^{-1}, having in mind the zone width where the temperature exceeds 401 °C.

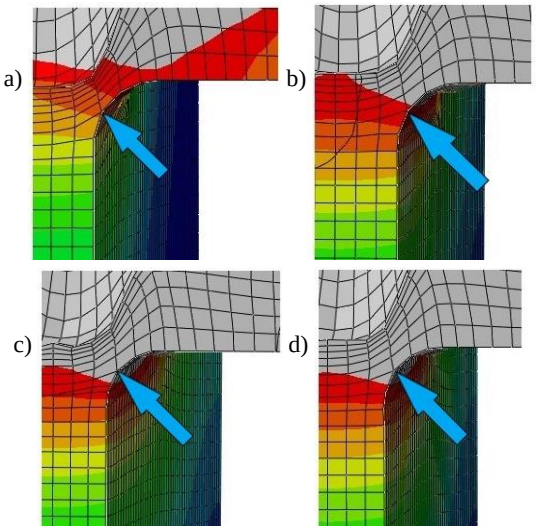

Figure 12. Temperature field after 28 s, pin length 2.6 mm (300, 500, 750, and 1000 min^{-1}, 0.1 m/s); same legend as in Fig. 10.

For the model with pin length 3 mm, it can be seen from Fig. 11 that tool rotation speed of 500 min^{-1} barely satisfies the temperature condition (401 °C) in the critical position. Therefore, equivalent von Mises stress field for this configuration is also considered, Fig. 13. It can be seen that stress values in the welding zone are relatively high; in order to present a closer view, detail A is marked in the figure, and shown in Fig. 14.

When stress values in this region obtained for different tool rotation speeds are compared, it can be seen that the stress values are very low, only for 750 and 1000 min^{-1}. This means that the temperature condition might not be sufficient to conclude that the adequate quality of the joint can be obtained. In other words, the material is still not soft enough for the tool rotation speed 500 min^{-1}.

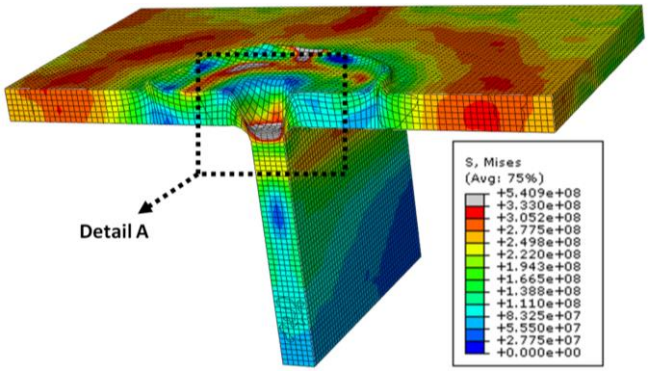

Figure 13. Equivalent von Mises stress field after 32 s, pin length 3 mm (500 min^{-1}, 0.1 m/s).

Results lead to the conclusion that an adequately welded and safe welded joint in the analysed configuration requires the tool with larger pin length, and pin geometry details will be analysed and optimised in future work.

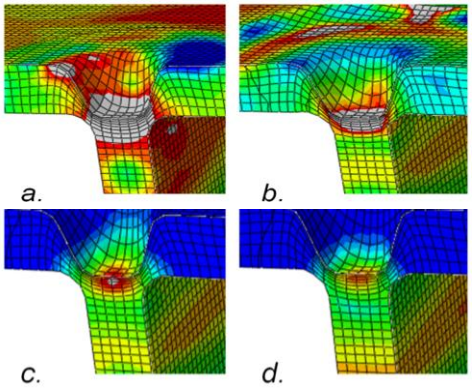

Figure 14. Equivalent von Mises stress field after 32 s, pin length 3 mm (300, 500, 750, and 1000 min^{-1}, 0.1 m/s), detail A; the same legend as in Fig. 13.

CONCLUSIONS

This work deals with the plunge stage of friction stir welding, i.e., the initial stage preceding the linear welding itself. However, it is of crucial importance to establish appropriate conditions during the tool plunging since inadequate heating will prevent correct joint formation. The most important findings can be summarized as follows:

- Temperature fields are symmetrical with respect to stringer plate middle plane.
- Increase of the tool rotation speed increases the temperature in the welding zone and creates conditions for eliminating the joining line.
- Increase of tool pin length contributes to the elimination of the joining line.
- Temperature condition revealed that the application of the tool of pin length 3 mm, tool rotation speed above 500 min^{-1} and tool penetration speed of 0.1 mm/s meets the conditions for successful welding of plates produced from Al alloy 2024 T3 in T-joint configuration. If the pin is 2.6 mm long, then the rotation speed of 750 min^{-1} is necessary.
- It is beneficial to analyse the stress field in the joint zone, in addition to temperature field; it is shown on the example of the model with pin length 3 mm.

ACKNOWLEDGEMENTS

This work was supported by the Ministry of Science, Technological Development and Innovation of the Republic of Serbia (contracts 451-03-66/2024-03/200287 and 451-03-65/2024-03/200135).

REFERENCES

1. Schmidt, H., Hattel, J. (2005), *A local model for the thermo-mechanical conditions in friction stir welding*, Modell. Simul. Mater. Sci. Eng. 13(1): 77-93. doi: 10.1088/0965-0393/13/1/006
2. Chen, C.M., Kovačević, R. (2003), *Finite element modeling of friction stir welding-thermal and thermomechanical analysis*, Int. J Mach. Tools Manuf. 43(13): 1319-1326. doi: 10.1016/S0890-6955(03)00158-5
3. He, X., Gu, F., Ball, A. (2014), *A review of numerical analysis of friction stir welding*, Progr. Mater. Sci. 65: 1-66. doi: 10.1016/j.pmatsci.2014.03.003
4. Mijajlović, M., Milčić, D., Milčić, M. (2014), *Numerical simulation of friction stir welding*, Therm. Sci. 18(3): 967-978. doi: 10.2298/TSCI1403967M

5. Çam, G., Javaheri, V., Heidarzadeh, A. (2023), *Advances in FSW and FSSW of dissimilar Al-alloy plates*, J Adhes. Sci. Technol. 37(2): 162-194. doi: 10.1080/01694243.2022.2028073
6. Sabry, I., El-Kassas, A.M., Mourad, A.-H.I., et al. (2019), *Friction stir welding of T-joints: experimental and statistical analysis*, J Manuf. Mater. Process. 3(2): 38. doi:10.3390/jmmp3020038
7. Cui, L., Yang, X., Xie, Y., et al. (2013), *Process parameter influence on defects and tensile properties of friction stir welded T-joints on AA6061-T4 sheets*, Mater. Des. 51: 161-174. doi: 10.1016/j.matdes.2013.04.013
8. Feistauer, E.E., Bergmann, L.A., dos Santos, J.F. (2018), *Effect of reverse material flow on the microstructure and performance of friction stir welded T-joints of an Al-Mg alloy*, Mater. Sci. Eng. A, 731: 454-464. doi: 10.1016/j.msea.2018.06.056
9. Đurđević, A., *Friction stir welding technology of aluminium alloy T joints* (in Serbian), PhD Thesis, University of Belgrade, Faculty of Mechanical Engineering, 2015.
10. Živković, A., Đurđević, A., Sedmak, A., et al. (2015), *Friction stir welding of aluminium alloys - T joints*, Struct. Integr. Life, 15(3): 181-186.
11. Aghajani Derazkola, H., Kordani, N., Aghajani Derazkola, H. (2021), *Effects of friction stir welding tool tilt angle on properties of Al-Mg-Si alloy T-joint*, CIRP J Manuf. Sci. Technol. 33: 264-276. doi: 10.1016/j.cirpj.2021.03.015
12. Jesus, J.S., Costa, J.M., Loureiro, A., Ferreira, J.M. (2018), *Assessment of friction stir welding aluminium T-joints. J*, Mater. Process. Tech. 255: 387-399. doi: 10.1016/j.jmatprotec.2017.12.036
13. Mertinger, V., Varbai, B., Adonyi, Y., et al. (2022), *Microstructure evaluation of dissimilar AA2024 and AA7050 aluminum joints made by corner stationary-shoulder friction stir welding*, Weld. World, 66: 1623-1635. doi: 10.1007/s40194-022-01321-5
14. Su, Y., Li, W., Liu, X., et al. (2021), *Evolution of microstructure, texture and mechanical properties of special friction stir welded T-joints for an α titanium alloy*. Mater. Charact. 177: 111152. doi: 10.1016/j.matchar.2021.111152
15. Su, Y., Li, W., Shen, J., et al. (2022), *Comparing the fatigue performance of Ti-4Al-0.005B titanium alloy T-joints, welded via different friction stir welding sequences*, Mater. Sci. Eng. A, 859: 144227. doi: 10.1016/j.msea.2022.144227
16. Kredegh, A., Sedmak, A., Grbović, A., et al. (2016), *Numerical simulation of fatigue crack growth in friction stir welded T joint made of Al 2024 T351 alloy*, Procedia Struct. Integr. 2: 3065-3072. doi: 10.1016/j.prostr.2016.06.383
17. Ambrosio, D., Wagner, V., Vivas, J. et al. (2023), *Advances in friction stir welding of Ti6Al4V alloy complex geometries: T-butt joint with complete penetration*, Archiv. Civ. Mech. Eng, 23: 182. doi: 10.1007/s43452-023-00717-4
18. Furkon, W.M., Kim, D.H., Song, M.Y. et al. (2022), *Effect of post-weld heat treatment on multi-scale microstructures and mechanical properties of friction stir welded T-joints of Al-Mg-Si alloys*, J Mater. Res. Technol. 18: 496-507. doi: 10.1016/j.jmrt. 2022.02.119
19. Salloomi, K.N. (2019), *Fully coupled thermomechanical simulation of friction stir welding of aluminum 6061-T6 alloy T-joint*, J Manuf. Process. 45: 746-754. doi: 10.1016/j.jmapro.2019.06.030
20. Wang, C., Deng, J., Dong, C., Zhao, Y. (2022), *Numerical simulation and experimental studies on stationary shoulder friction stir welding of aluminum alloy T-joint*, Front. Mater. 9: 898929. doi: 10.3389/fmats.2022.898929
21. Campanella, D., Buffa, G., Lamia, D., Fratini, L. (2022), *Residual stress and material flow prediction in friction stir welding of Gr2 titanium T-joints*, Manuf. Lett. 33: 249-258.
22. Ameur, S., El Bahri, C.O., Djebli, A., et al. (2021), *Analysis of FSW parameters: numerical simulation of HDPE plate*, Struct. Integr. Life, 21(3): 301-308.
23. Aghajani Derazkola, H., Simchi, A. (2019), *An investigation on the dissimilar friction stir welding of T-joints between AA5754 aluminum alloy and poly(methyl methacrylate)*, Thin-Wall. Struct. 135: 376-384. doi: 10.1016/j.tws.2018.11.027
24. Beygi R., Abbas Talkhabi A., Zarezadeh Mehrizi M., et al. (2023), *A novel lap-butt joint design for FSW of aluminum to steel in tee-configuration: joining mechanism, intermetallic formation, and fracture behavior*, Metals, 13(6): 1027. doi: 10.3390/met13061027
25. Ali, M., Anjum, S., Noor Siddiquee, A., et al. (2020), *Defect formation during dissimilar aluminium friction stir welded T-joints*, Mech. Industry, 21(2): 205. doi: 10.1051/meca/2020005
26. Certificate Conformity, ALCOA International, Inc., Approved Certificate No. 47831, 1990.
27. ASM International Aluminum 2024-T351 Data Sheet
28. Johnson, G.R., Cook, W.H. (1983), *A constitutive model and data for metals subjected to large strains, high strain rates and high temperatures*, In: Proc. Seventh Int. Symp. on Ballistics, The Hague, The Netherlands, pp.541-547.
29. Veljić, D., Rakin, M., Perović, M., et al. (2013), *Heat generation during plunge stage in friction stir welding*, Therm. Sci. 17(2): 489-496. doi: 10.2298/TSCI120301205V
30. Veljić, D., Međo, B., Rakin, M., et al. (2016), *Analysis of the tool plunge in friction stir welding - comparison of aluminium alloys 2024 T3 and 2024 T351*, Therm. Sci. 20(1): 247-254. doi: 10.2298/TSCI150313059V
31. Veljić, D., Perović, M., Sedmak, A., et al. (2011), *Numerical simulation of the plunge stage in friction stir welding*, Struct. Integr. Life, 11(2): 131-134.
32. Ivanović, I., Sedmak, A., Miloš, M., et al. (2011), *Numerical study of transient three-dimensional heat conduction problem with a moving heat source*, Therm. Sci. 15(1): 257-266. doi: 10.2298/TSCI1101257I
33. Sedmak, A., Kumar, R., Chattopadhyaya, et al. (2016), *Heat input effect of friction stir welding on aluminum alloy AA 6061-T6 welded joint*, Therm. Sci. 20(2): 637-641. doi: 10.2298/TSCI150814147D
34. Veljić, D., Rakin, M., Sedmak, A., et al. (2022), *Thermo-mechanical analysis of linear welding stage in friction stir welding: Influence of welding parameters*, Therm. Sci. 26(3A): 2125-2134. doi: 10.2298/TSCI210216186V
35. Veljić, D., Rakin, M., Međo, B., et al. (2019), *Temperature fields in linear stage of friction stir welding: Effect of different material properties*, Therm. Sci. 23(6B): 3985-3992. doi: 10.2298/TSCI181015264V
36. Veljić, D., Radović, N., Rakin, M., et al. (2023), *Influence of temperature and plastic deformation on AA2024 T3 friction stir welded joint microstructure*, Therm. Sci. 27(1A): 311-320. doi: 10.2298/TSCI220621162V
37. Murray, J.L. (1982), *The Al-Mg (Aluminum-Magnesium) system*, Bull. Alloy Phase Diagr. 3: 60-74. doi: 10.1007/BF02873413
38. Balawender, T., Myśliwiec, P. (2020), *Experimental analysis of FSW process forces*, Adv. Manuf. Sci. Tech. 44(2): 90-95. doi: 10.2478/amst-2019-0006
39. Zhang, H., Lin, S.B., Wu, L., et al. (2006), *Defects formation procedure and mathematic model for defect free friction stir welding of magnesium alloy*, Mater. Des. 27(9): 805-809. doi: 10.1016/ j.matdes.2005.01.016